Eur. Phys. J. A (2023) 59:182
https://doi.org/10.1140/epja/s10050-023-01094-5

THE EUROPEAN PHYSICAL JOURNAL A

Regular Article - Theoretical Physics

Effects of deuteron breakup and nucleon-transfer reactions on d+^{11}B elastic scattering

A. Amar[1], **K. Rusek**[2], **Sh. Hamada**[1,a]

[1] Faculty of Science, Tanta University, Tanta, Egypt
[2] Heavy Ion Laboratory, University of Warsaw, ul. L. Pasteura 5A, 02-093 Warsaw, Poland

Received: 30 April 2023 / Accepted: 18 July 2023 / Published online: 8 August 2023

Communicated by Arnau Rios Huguet

Abstract A set of experimental data consisting of angular distributions of d+^{11}B elastic and inelastic scattering and (d,t) reaction obtained at deuteron energy of 14.5 MeV as well as data sets for (d,p) (E_d = 21.5 MeV), (d,n) (E_d = 15.4 MeV) and (d,^{3}He) (E_d = 11.8 MeV) nucleon transfer reactions were analysed using the continuum-discretized coupled-channel (CDCC) and coupled-reaction channel (CRC) methods. It was found that at forward scattering angles the elastic scattering data are well described by parameter-free CDCC calculations which include breakup of the deuteron, but at more backward angles virtual effects due to target excitation and neutron-transfer reactions play an important role. The strongest effects are due to the excitation of ^{11}B and the neutron pickup reaction, reflecting their large cross sections. The effects induced by proton-transfer reactions are found to be negligible.

1 Introduction

The deuteron, a bound system of the proton and the neutron, is one of the simplest nuclei, having no bound or resonant excited states. However, due to its small binding energy, large size and large spectroscopic quadrupole moment, reactions induced by deuterium beams have attracted much attention. Progress in deuteron breakup studies came with the CDCC method, introduced by Rawitscher [1] and developed especially by the Kyushu group and used in analyses of many data sets [2,3]. The method has become a standard tool for analyses of reactions induced by weakly bound exotic isotopes at low energy and is still being developed [4]. A large set of deuteron elastic scattering data analysed within the CDCC method was published quite recently by Chau Huu-Tai [5].

For light targets, the low energy deuteron elastic scattering data were well reproduced at forward scattering angles by CDCC calculations [5], showing that the virtual effects of breakup are important there. However, at more backward angles the difference between predictions and measurements was sizable, suggesting couplings with other direct reaction channels. Studies of transfer reactions induced by deuterons and their effect on elastic scattering have been performed for a long time, some quite recent results can be found in [6–9]. In Ref. [10], it was found that the (d,p) reaction has a significant effect on d+^{16}O elastic scattering at 11 MeV, with a tendency to decrease with increasing energy. The effect of breakup also decreases with energy, but more slowly. Upadhyay et al. [8] studied deuteron induced reactions on ^{10}Be, ^{12}C and ^{48}Ca at energies from 12 to 71 MeV showing that the elastic scattering data can be described by coupling to breakup of the deuteron and the (d,p) stripping reaction. The contributions of (d,t) and (d,^{3}He) pickup reactions on d+^{40}Ca elastic scattering at 52 MeV were found to be important at scattering angles larger than 40 deg by Keeley and Mackintosh [7].

In the present paper, a recently published data set for deuteron induced reactions on a ^{11}B target at 14.5 MeV [11], together with previously published data sets for (d,p) [12], (d,n) [14] and (d,^{3}He) [13] reactions on a ^{11}B target at similar energies are analysed by means of the CDCC and CRC methods in order to establish to what extent the elastic scattering data are affected by virtual couplings with the breakup and reaction processes.

All the calculations presented in this paper were performed using the computer code Fresco [15].

[a] e-mail: sh.m.hamada@science.tanta.edu.eg (corresponding author)

Table 1 Parameters of the W-S potentials

	V_r MeV	r_o fm	a_o fm	W_v MeV	W_s MeV	r_w fm	a_w fm	Ref.
n+^{11}B	47.1	1.31	0.660	0.0	8.38	1.260	0.480	[18]
p+^{11}B	50.0	1.13	0.700	13.3	0.0	1.130	0.700	[19]
p+^{12}B	64.97	1.006	0.654	0.0	4.613	1.321	0.702	[12]
t+^{10}Be	116.82	1.077	0.820	0.0	2.00	1.25	0.840	[26]
^{3}He+^{10}B	119.9	1.002	0.820	2.17	7.1	1.25	0.840	[26]
n+^{12}C	50.48	1.150	0.689	1.77	8.26	1.146	0.689	[14]

For the definition see Ref. [26]. Radii are defined according to the light ion convention, $R_{o,w} = r_{o,w} A_T^{1/3}$

2 Effect of deuteron breakup on elastic scattering

The CDCC method was used to study the deuteron breakup in the d+^{11}B system at 14.5 MeV. The potential binding the neutron and proton was of Gaussian form,

$$V_{pn} = V_0 exp(-r/r_0)^2,$$

with r_0 = 1.484 fm [3,17]. The ground state wave function of the deuteron consisted of S- and D-components [16] calculated in the potential well with depth parameter V_0 = 72.15 MeV or 515.26 MeV, respectively. The depth parameter V_0 was chosen so that the binding energy of the deuteron (2.2246 MeV) was reproduced. Choice of the spectroscopic amplitudes, 0.9706 for the S-component and 0.2410 for the D-component, allowed reproduction of the spectroscopic quadrupole moment of the deuteron. This choice of the *n*-*p* binding potential is not unique. One can use, for example, Woods-Saxon potential and obtain similar results to those presented in this paper.

The momentum (k) space above the $d \rightarrow n, p$ breakup threshold was truncated at k_{max} = 0.5 fm^{-1} (E_{max} = 10.45 MeV), corresponding to the energy of the incoming deuteron (the contribution of the so-called "closed channels" was ignored), and divided into momentum bins of equal width, Δk = 0.125 fm^{-1} [6,17]. Only states with L=0,2 were included as the effect of L = 1,3 states on the final results was found to be negligible. The convergence of the calculations was proven in a series of test runs. The test calculations also showed that the effect of the D-state component of the deuteron ground state wave function (effect of the deuteron quadrupole moment) on the calculated cross sections was negligible.

All the interaction potentials were derived using the standard single-folding technique [1] from empirical optical model (OM) potentials describing elastic scattering of neutrons and protons from ^{11}B [18,19]. The parameters of the potentials are listed in Table 1. For the d+^{11}B scattering at 14.5 MeV these potentials should be taken at approximately half this energy [1]. However, the potentials found in the literature correspond to larger energies—that for n+^{11}B to 9.7 MeV and for p+^{11}B to 17 MeV. As a concequence, one should expect that CDCC calculations with these input potentials will need to be adjusted in order to fit the experimental results.

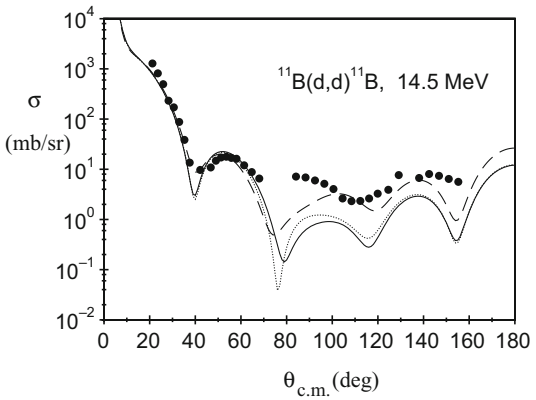

Fig. 1 Angular distribution of the d+^{11}B elastic scattering differential cross section. The solid curve shows results of CDCC calculations, while the dashed curve the one-channel calculations, with coupling to the breakup channels omitted. The optical model calculations with the effective potential (see text) are presented by the dotted curve

The results of the (free from any adjustable parameter) CDCC calculations are plotted as the solid curve in Fig. 1. As in some earlier studies mentioned above, they describe well the experimental data of elastic scattering at forward scattering angles, up to about 70 deg in the centre of mass system. At more backward angles the calculations underestimate the measured values of the differential cross section.

The dashed curve in Fig. 1 presents the result of a one-channel calculation, with only the ground state of the deuteron included. The comparison with the full CDCC result shows that the deuteron breakup induces a significant reduction of the elastic scattering differential cross section at scattering angles larger than 70 deg. A similar effect was observed for other scattering systems, e.g. d+^{58}Ni [2] and d+^{11}Be [20] but in those studies one-channel calculations overestimated the elastic scattering data. This comparison therefore suggests a need for a reduction of the imaginary terms in the input n, p+^{11}B optical potentials. In the d+^{40}Ca study [7],

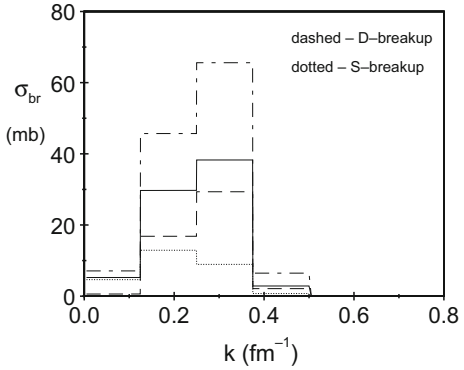

Fig. 2 Dependence of the breakup cross section on the $p-n$ relative momentum k. The histogram plotted by the solid line corresponds to the total breakup c.s., while the dashed and dotted lines show its components, as indicated in the figure. The total breakup c.s. calculated with the reduced imaginary parts of the input n, p+^{11}B optical potentials is plotted by the dotdashed line

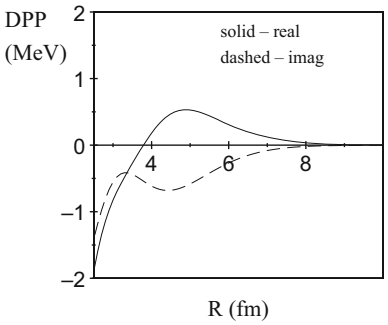

Fig. 3 Dynamic polarization potential (DPP) representing the CDCC calculations as a function of d-^{11}B separation

the imaginary terms of the input potentials were reduced by 30% in order to obtain the best possible description of the elastic scattering data.

The CDCC calculations yielded a total breakup cross section of 76 mb, dominated by the contribution of the continuum D states (Fig. 2). Similar dominance of the couplings to the D-states from the $n-p$ continuum was observed by Yahiro et al. [2] for the deuteron breakup on ^{58}Ni. The strengh of the imaginary n, p+target input potentials affects the value of the calculated total breakup cross section, as shown in [2] and quoted in [3]. This was also observed in the present study, a reduction of the imaginary parts of the input potentials by 35% increased the value of the breakup cross section to 125.3 mb. Results of the CDCC calculations with such a reduction of the imaginary potential strength are plotted in Fig. 5 by the dotted curve.

A dynamic polarization potential (DPP) may be derived from the CDCC calculations using the trivially equivalent method [21] or by an inversion of the S-matrix [7]. When added to the *bare* single-folding potential it forms an effective potential that should reproduce the angular distribution of the elastic scattering cross section in a simple optical model (OM) calculation, giving results close to those obtained with the CDCC calculations. Such a DPP potential, obtained in this study using the trivially equivalent method [21], is plotted in Fig. 3. It consists of a real part, repulsive at the nuclear surface, and an imaginary part increasing the absorption at the surface. This is a typical DPP, observed for many scattering systems, for example for d+^{58}Ni breakup at 56 MeV [2,3] and for the breakup of other weakly bound projectiles at energies well above the Coulomb barrier [22].

Optical model calculations with the effective potential obtained in this work yielded results very close to the original CDCC (see the comparison of the dotted and solid curves in Fig. 1). So the deuteron breakup effects could be well simulated by means of such a potential. In the further studies described below, which included couplings with the ^{11}B excitation and with the nucleon-transfer reactions, such a potential, obtained from CDCC calculations, was used in the entrance d+^{11}B channel. This approximation greatly facilitated the calculations but excluded from the study effects related to direct coupling of the processes listed above with the deuteron breakup channels. Note, that using this approximation any OM potential giving similar d+^{11}B elastic scattering cross sections should give also similar results for the reaction channels.

A comprehensive review of the theoretical methods used to describe deuteron induced reactions was recently published by Timofeyuk and Johnson [23]. One of the alternative methods that could be applied for the present analysis is the Adiabatic Distorted Wave Approximation (ADWA) that is using the formalism developed by Johnson and Tandy [24] allowing for the d-breakup degrees of freedom to be included. It was shown that at low incident energies (like in this paper) the ADWA and CDCC methods give very close results for ^{10}Be(d,p)^{11}Be reaction [23,25].

3 Effects due to target excitation and nucleon transfer reactions

3.1 Coupled Channel calculations for ^{11}B excitation

In the d+^{11}B experiment of Nassurlla et al. [11] inelastic scattering leading to the two excited states of ^{11}B at 4.45 MeV and 6.74 MeV was measured. These states are often considered as members of K = 3/2 rotational band built on the ^{11}B ground state [11]. However, as the Coriolis term is able to mix configurations having the same angular momentum but which differ in K, the assumption that these three states are pure K = 3/2 rotational states should be considered as a rough approximation [27,28]. Nevertheless, in the present study this approximation was used, with the nuclear defor-

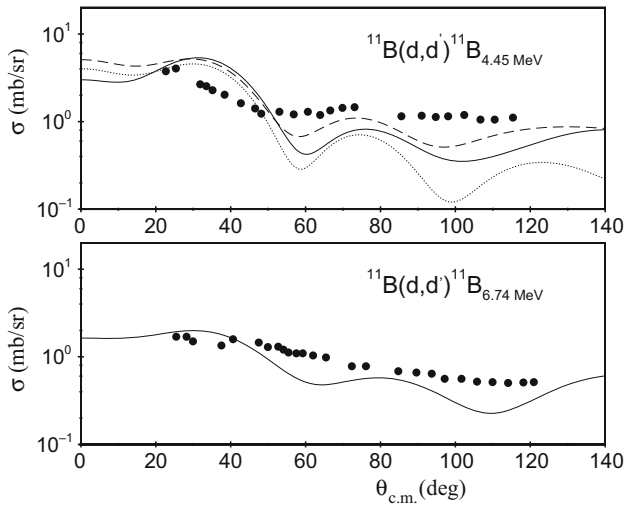

Fig. 4 Comparison of d+^{11}B inelastic scattering data leading to the two excited states of ^{11}B, with the CC (dotted and dashed curves) and CRC (solid curve) calculations. More details in the text

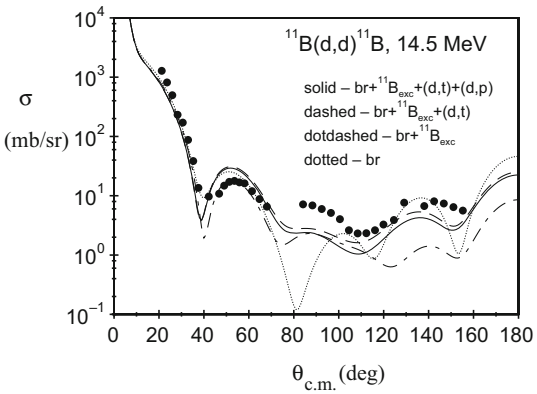

Fig. 5 Comparison of d+^{11}B elastic scattering data with the model calculations including various processes. CDCC calculations were performed with the imaginary parts of the input potentials reduced by 35 percent and in all other calculations an effective potential corresponding to this CDCC result was used

mation lengh $\delta = 2.5$ fm corresponding to a quadrupole deformation parameter of $\beta = 0.8$ [11,28] and a Coulomb deformation parameter derived from the spectroscopic quadrupole moment of the ^{11}B ground state [29].

Coupled channel (CC) calculations involving quadrupole rotational couplings among the three states (g.s., 4.45 MeV and 6.74 MeV), with the effective potential corresponding to the CDCC calculations presented in Fig. 1, led to a rather poor description of the measured inelastic scattering angular distributions. An example is shown in Fig. 4 by the dotted curve for the 4.45 MeV state. A better description was obtained with the potential derived from the CDCC calculations with the imaginary parts of the input OM potentials reduced by 35% and this is plotted by the dotted curve in Fig. 5 (dashed curve in Fig. 4). In the further study, described below, this reduced effective potential was used.

Table 2 Spectroscopic factors used in the CRC calculations

	NLJ	S_A	Ref.
^{3}H = d+n	1S1/2	1.5	[30]
^{3}He = d+p	1S1/2	1.5	[30]
$^{11}B_{g.s.}$ = $^{10}B_{g.s.}$+n	1P3/2	1.44	This work
$^{11}B_{g.s.}$ = $^{10}B_{0.718MeV}$+n	1P1/2	0.44	This work
$^{11}B_{g.s.}$ = $^{10}B_{0.718MeV}$+n	1P3/2	0.07	This work
$^{11}B_{g.s.}$ = $^{10}B_{2.15MeV}$+n	1P2/3	0.36	This work
$^{12}B_{g.s.}$ = $^{11}B_{g.s.}$+n	1P1/2	0.69	[32]
$^{12}B_{1.67\ MeV}$ = $^{11}B_{g.s.}$+n	2S1/2	0.33	[32]
$^{12}B_{2.62\ MeV}$ = $^{11}B_{g.s.}$+n	2S1/2	0.63	[32]
$^{12}C_{g.s.}$ = $^{11}B_{g.s.}$+p	1P3/2	2.16	This work
$^{11}B_{g.s.}$ = $^{10}Be_{g.s.}$+p	1P3/2	0.64	[31]

The effect of the target excitation on the elastic scattering is illustrated in Fig. 5. The dotted curve shows the result of CDCC calculation while the dotdashed curve plots the result of the CC calculation. Inclusion of the target excitation fills the oscillation of the dotted cuve at about 80 deg and reduces the elastic scattering cross section at about 140 deg. Moreover, the shape of the calculated angular distribution becomes closer to the experimental one.

3.2 ^{11}B(d,t)^{10}B reaction

In order to study the influence of the (d,t) pickup reaction on the elastic scattering, the data obtained by Nassurlla et al. [11] were used. The data set, consisting of three angular distributions of emitted tritons, corresponding to the g.s., 0.718 MeV and 2.15 MeV states of ^{10}B, was reanalysed in the present paper by means of the CRC method. As mentioned above, in the d+^{11}B entrance channel the reduced effective potential, simulating effects of deuteron breakup, was applied.

The important point of the analysis was the choice of the exit channel potential for t+^{10}B. This scattering system has not been investigated at the required energy. Thus, in the present analysis a global triton OM potential [26] was applied, with the depth of its imagnary part adjusted in order to obtain the best description of the ^{11}B(d,t)$^{10}B_{g.s.}$ experimental data by the CRC calculation. The parameters of the t+^{10}B OM potential obtained this way are listed in the Table 1. All the binding potentials were of the standard WS form, with geometry parameters $r_0 = 1.25$ fm, $a_0 = 0.65$ fm and the depths adjusted to get the proper binding energies. The spectroscopic factor for the triton ground state was taken from the shell model calculations of Rudchik and Tchuvilsky [30]. All the spectroscopic factors used in the present work are listed in Table 2.

Inclusion of the neutron pickup reaction in the CRC coupling scheme significantly affected the results for elastic scattering at backward angles (see the comparison of results plotted with the dashed and dotdashed curves on Fig. 5, reducing the difference between the elastic scattering data and the model predictions at backward scattering angles.

3.3 ^{11}B(d,p)^{12}B neutron stripping reaction

In the next step, the (d,p) reaction was added to the coupling scheme. Experimental data for this process were measured at lower [12] and higher energies [32]. In the the present CRC calculations, transitions to three states of ^{12}B were included (g.s., 1.67 MeV and 2.62 MeV). The geometry of the ^{11}B+n binding potential and corresponding spectroscopic factors were adopted from the studies of Belyaeva et al. [32]. In the exit p+^{12}B channel the energy-dependent OM potential proposed in Ref. [12] was used. Test calculations performed at a deuteron energy of 21.5 MeV showed reasonable agreement with the transfer data of Belyaeva [32].

Results of the CRC calculations including ^{11}B excitation to the 4.45 MeV and 6.74 MeV states, neutron pickup to the g.s, 0.718 MeV and 2.15 MeV states of ^{10}B and neutron stripping to the g.s., 1.67 MeV and 2.62 MeV states of ^{12}B are plotted as the solid curves in Figs. 4, 5, 6. The description of the experimental data is far from perfect, nevertheless the calculated relative contributions to the elastic channel should reflect real effects. The small difference between the dashed and solid curves in Fig. 5 shows that the effect of the neutron stripping (d,p) reaction is much smaller than the effects due to deuteron breakup, target excitation and (d,t) neutron pickup, confirming the conclusions derived from the d+^{40}C study presented in Ref. [7].

3.4 ^{11}B(d,^{3}He)^{10}Be and ^{11}B(d,n)^{12}C reactions

For completeness, the effects on the elastic scattering induced by the p-pickup and p-stripping reactions were studied with the help of the data presented in the papers of Fitz et al. [13] and Febbraro et al. [14].

In Ref. [13], the angular distribution of ^{3}He emerging from the proton pick-up reaction induced by an 11.8 MeV deuteron beam on a ^{11}B target and leading to the ground state of ^{10}Be was measured and analyzed by means of the distorted wave Born approximation (zero range) method. In the present paper, these data were reanalyzed using the CRC method. In the exit channel the ^{3}He+^{10}Be OM potential was adopted from the Fitz et al. study [13] (Table 1). The binding potentials for ^{3}He and ^{11}B wave functions were taken to be of WS form, with standard geometry parameters, r_0 = 1.25 fm and a_0 = 0.65 fm, and the respective spectroscopic amplitudes were taken from shell model predictions [30,31] (Table 2).

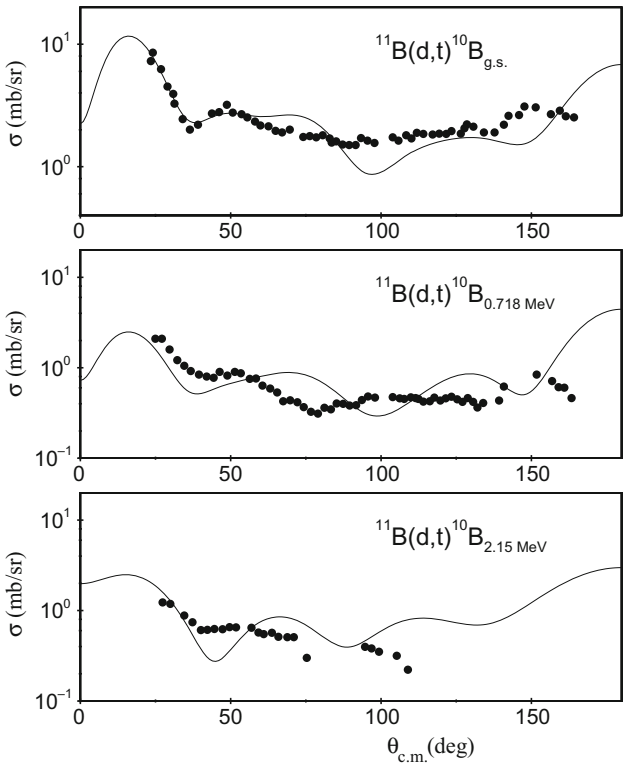

Fig. 6 Comparison of the experimental data corresponding to the (d,t,) reaction leading to the three states of ^{10}B with the CRC calculations. The solid curves represent calculations including target excitation, (d,t) and (d,p) reactions

Test calculations at 11.8 MeV revealed good agreement with the experimental data of Ref. [13].

For the proton stripping reaction, ^{11}B(d,n)^{12}C, the experimental data published by Febbraro et al. [14] were reanalysed using the CRC method, with the OM potential in the exit channel adopted from global predictions [33] and the spectroscopic factor for $^{12}C_{g.s.}$ adjusted in order to obtain the best possible reproduction of the experimental data of Ref. [14].

Both p-transfer processes are characterized by relatively small cross sections and their influence on the elastic scattering was found to be negligible.

4 Summary

Various processes induced by deuterons incident on ^{11}B: elastic scattering, d-breakup, excitation of the target nucleus and n- and p- transfer reactions were studied by means of the CDCC and CRC methods. The influence of the inelastic processes on the elastic scattering was estimated.

It was found that CDCC calculations, taking into account the loosely bound structure of the deuteron, are able to describe the angular distribution of the elastic scattering at

forward scattering angles without any adjustable parameter. At backward scattering angles the inelastic processes like target excitation and nucleon-transfer reactions significantly modify the CDCC results. Moreover, at these angles, the imaginary parts of the input nucleon-target OM potentials also play an important role. Thus, this kind of study requires a precise knowledge of the nucleon-target interactions at the required energy. For light targets and low energies the existing global nucleon-target OM potentials do not provide precise enough predictions. CDCC calculations have shown a dependence of the calculated deuteron breakup cross section on the imaginary parts of the input nucleon-target OM potentials. Comparison of the calculated results with the experimental values can serve as a criterion for the choice of the strengths of these parts.

Apart from breakup, two inelastic processes, target excitation and the neutron pickup reaction, were found to affect mostly the elastic scattering at backward angles. An effect from neutron stripping was also encountered, while the virtual processes due to proton-transfer reactions contributed negligibly to the elastic scattering.

Some other observations can be summarized as follows. Breakup of the deuteron reduces the elastic scattering differential cross section at backward angles in comparison with the OM calculations employing a single-folding potential. The contribution related to the quadrupole moment of the deuteron ground state is negligibly small in comparison with the contribution generated by couplings to the states from the $n - p$ continuum. The effect of target excitation on the elastic scattering cross section is similar in character to that of the breakup. However, coupling to the neutron-transfer reactions acts in the opposite way, increasing the elastic scattering cross section at backward scattering angles better to match the data.

Acknowledgements We are grateful to Professor Nicholas Keeley for reading the manuscript and for helpful suggestions. A. Amar and Sh. Hamada are funded from the Ministry of Higher Education of the Arab Republic of Egypt by a full postdoctoral scholarship.

Funding Open access funding provided by The Science, Technology &; Innovation Funding Authority (STDF) in cooperation with The Egyptian Knowledge Bank (EKB).

Data availability statement The manuscript has associated data in a data repository. [Author's comment: The experimental data used in the present study was published by M. Nassurlla et al., Nucl. Phys. A **1023**, 122448 (2022). https://doi.org/10.1016/j.nuclphysa.2022.122448.]

References

1. H.G. Rawitscher, Phys. Rev. C **9**, 2210 (1974). https://doi.org/10.1103/PhysRevC.9.2210
2. M. Yahiro et al., Prog. Theor. Phys. Supp. **89**, 32 (1986). https://doi.org/10.1143/PTPS.89.32
3. N. Austern et al., Phys. Rep. **154**, 125 (1987). https://doi.org/10.1016/0370-1573(87)90094-9
4. C.W. Johnson et al., J. Phys. G **47**, 123001 (2020). https://doi.org/10.1088/1361-6471/abb129
5. P. Chau Huu-Tai, Nucl. Phys. A **773**, 56 (2006). https://doi.org/10.1016/j.nuclphysa.2006.04.006
6. N. Keeley, N. Alamanos, V. Lapoux, Phys. ReV. C **69**, 064604 (2004). https://doi.org/10.1103/PhysRevC.69.064604
7. N. Keeley, R.S. Mackintosh, Phys. Rev. C **77**, 054603 (2008). https://doi.org/10.1103/PhysRevC.77.054603
8. N.J. Upadhyay, A. Deltuva, F.M. Nunes, Phys. Rev. C **85**, 054621 (2012). https://doi.org/10.1103/PhysRevC.85.054621
9. R.S. Mackintosh, N. Keeley, Phys. Rev. C **76**, 024601 (2007). https://doi.org/10.1103/PhysRevC.76.024601
10. M. Kawai, M. Kamimura, K. Takesako, Prog. Theor. Phys. Supp. **89**, 118 (1986). https://doi.org/10.1143/PTPS.89.118
11. M. Nassurlla et al., Nucl. Phys. A **1023**, 122448 (2022). https://doi.org/10.1016/j.nuclphysa.2022.122448
12. Z.H. Liu et al., Phys. Rev. C **64**, 034312 (2001). https://doi.org/10.1103/PhysRevC.64.034312
13. W. Fitz, R. Jahr, R. Santo, Nucl. Phys. A **101**, 449 (1967). https://doi.org/10.1016/0375-9474(67)90198-4
14. M. Febbraro et al., Phys. Rev. C **96**, 024613 (2017). https://doi.org/10.1103/PhysRevC.96.024613
15. I.J. Thompson, Comput. Phys. Rep. **7**, 167 (1988). https://doi.org/10.1016/0167-7977(88)90005-6
16. M. Lacombe et al., Phys. Rev. C **21**, 861 (1980). https://doi.org/10.1103/PhysRevC.21.861
17. Y. Iseri, M. Yahiro, M. Kamimura, Prog. Theor. Phys. Supp. **89**, 84 (1986). https://doi.org/10.1143/PTPS.89.84
18. J.A. Cookson, J.G. Locke, Nucl. Phys. A **146**, 417 (1970). https://doi.org/10.1016/0375-9474(70)90735-9
19. H.G. Pugh et al., Phys. Rev. **155**, 1054 (1967). https://doi.org/10.1103/PhysRev.155.1054
20. P. Descouvement, Phys. Rev. C **97**, 064607 (2018). https://doi.org/10.1103/PhysRevC.97.064607
21. M.A. Franey, P.J. Ellis, Phys. Rev. C **23**, 787 (1981). https://doi.org/10.1103/PhysRevC.23.787
22. Y. Sakuragi, M. Yahiro, M. Kamimura, Prog. Theor. Phys. Supp. **89**, 136 (1986). https://doi.org/10.1143/PTPS.89.136
23. N.K. Timofeyuk, R.C. Johnson, Prog. Part. Nucl. Phys. **111**, 103738 (2022). https://doi.org/10.1016/j.ppnp.2019.103738
24. R.C. Johnson, P.C. Tandy, Nucl. Phys. A **235**, 56 (1974). https://doi.org/10.1016/0375-9474(74)90178-X
25. N.J. Upadhyay, A. Deltuva, F.M. Nunes, Phys. Rev. C **85**, 054621 (2012). https://doi.org/10.1103/PhysRevC.85.054621
26. D.Y. Pang et al., Phys. Rev. C **79**, 024615 (2009). https://doi.org/10.1103/PhysRevC.79.024615
27. J.F. Cavaignec, S. Jang, D.H. Worledge, Nucl. Phys. A **243**, 349 (1975). https://doi.org/10.1016/0375-9474(75)90253-5
28. S. Mezhevych, PhD Thesis, Andrzej Soltan Inst. for Nuclear Studies, Warsaw (2002), unpublished

29. F. Ajzenberg-Selove, Nucl. Phys. A **506**, 1 (1990). https://doi.org/10.1016/0375-9474(90)90271-M
30. A.T. Rudchik, Yu.M. Tchuvilsky, Ukr. Fiz. Zh. **30**, 819 (1985)
31. S. Cohen, D. Kurath, Nucl. Phys. A **101**, 1 (1967). https://doi.org/10.1016/0375-9474(67)90285-0
32. T.L. Belyaeva et al., Phys. Rev. C **98**, 034602 (2018). https://doi.org/10.1103/PhysRevC.98.034602
33. R.L. Varner et al., Phys. Rep. **201**, 57 (1991). https://doi.org/10.1016/0370-1573(91)90039-O